Neuron, Vol. 41, 755–766, March 4, 2004, Copyright ©2004 by Cell Press

Streamlined Synaptic Vesicle Cycle in Cone Photoreceptor Terminals

Ruth Rea,[1] Jian Li,[2] Ajay Dharia,[1] Edwin S. Levitan,[3] Peter Sterling,[2] and Richard H. Kramer[1,*]
[1]Department of Molecular and Cell Biology
Division of Neurobiology
University of California at Berkeley
Berkeley, California 94720
[2]Department of Neuroscience
University of Pennsylvania School of Medicine
Philadelphia, Pennsylvania 19104
[3]Department of Pharmacology
University of Pittsburgh
Pittsburgh, Pennsylvania 15261

Summary

Cone photoreceptors tonically release neurotransmitter in the dark through a continuous cycle of exocytosis and endocytosis. Here, using the synaptic vesicle marker FM1-43, we elucidate specialized features of the vesicle cycle. Unlike retinal bipolar cell terminals, where stimulation triggers bulk membrane retrieval, cone terminals appear to exclusively endocytose small vesicles. These retain their integrity until exocytosis, without pooling their membranes in endosomes. Endocytosed vesicles rapidly disperse through the terminal and are reused with no apparent delay. Unlike other synapses where most vesicles are immobilized and held in reserve, only a small fraction (<15%) becomes immobilized in cones. Photobleaching experiments suggest that vesicles move by diffusion and not by molecular motors on the cytoskeleton and that vesicle movement is not rate limiting for release. The huge reservoir of vesicles that move rapidly throughout cone terminals and the lack of a reserve pool are unique features, providing cones with a steady supply for continuous release.

Introduction

Vertebrate photoreceptors tonically release neurotransmitter in the dark. To achieve a continuous cycle of exocytosis and endocytosis necessary for tonic release, the photoreceptor terminal has functional and structural specializations. Exocytosis is unusually sensitive to Ca^{2+} (Rieke and Schwartz, 1996), and vesicles are released at an unusually high rate in the dark, allowing small changes in light intensity to generate significant changes in neurotransmitter release (Ashmore and Copenhagen, 1983; Rao-Mirotznik et al., 1998). Endocytosis occurs with an unusually short delay after a rise in Ca^{2+}, rapidly and accurately retrieving membrane added by exocytosis (Rieke and Schwartz, 1996). The photoreceptor terminal has synaptic ribbons, the key structural specialization that allows rapid and coordinated exocytosis and endocytosis (for review, see von Gersdorff and Matthews, 1999; Fuchs et al., 2003). Here we ask whether, in addition to exocytosis and endocytosis, other steps in the vesicle cycle are also specialized for continuous release in cone photoreceptors.

At conventional phasic synapses that release transmitter during action potentials, the routes of vesicle recycling are often direct. This can include rapid reuse, where endocytosed vesicles are preferentially rereleased (Ceccarelli et al., 1973; Murthy and Stevens, 1998; Pyle et al., 2000; Richards et al., 2003), and kiss-and-run exocytosis, where docked vesicles release multiple times while remaining attached to the plasma membrane (Klingauf et al., 1998; Stevens and Williams, 2000; Gandhi and Stevens, 2003; Aravanis et al., 2003). However, there are also detours in the vesicle cycle, where retrieved membrane is stored and perhaps processed before reuse. For example, during endocytosis, recycling can occur through bulk membrane retrieval, resulting in large vacuoles that eventually give rise to new synaptic vesicles (Takei et al., 1996; Richards et al., 2000; Teng and Wilkinson, 2000). Moreover, small internalized vesicles may be recycled by first fusing with intracellular endosomes from which new vesicles are born (Heuser and Reese, 1973; Ryan et al., 1996), especially during intense stimulation (Richards et al., 2003). Finally, at conventional synapses only a small minority of vesicles is "readily releasable" (for review, see Zucker and Regehr, 2002). Most are relatively distant from release sites and immobilized by being tethered to the cytoskeleton by proteins such as synapsin (Hilfiker et al., 1999). These "reserve vesicles" are resistant to release and only slowly equilibrate with the readily-releasable pool. Hence, a large fraction of synaptic membrane is side tracked from participating in the vesicle cycle.

The vesicle cycle at ribbon synapses has been studied primarily in the retinal bipolar cell, which like photoreceptors contain hundreds of thousands of synaptic vesicles and employ graded release (Lagnado et al., 1996; von Gersdorff et al., 1996). However, release from the bipolar cell has a strong phasic component. Step depolarization triggers a transient burst of release (6000 vesicles released over 200 ms) followed by a dramatic slowing, suggesting exhaustion of a readily-releasable pool that refills only after tens of seconds (von Gersdorff and Matthews, 1997, 1999). Tracer studies show that actively cycling vesicles remain within 1 μm of the plasma membrane (Lagnado et al., 1996; Paillart et al., 2003). Sustained stimulation eventually labels reserve vesicles in the center of the bipolar terminal that appear immobile and resistant to release (Lagnado et al., 1996), although recent studies challenge this view (Holt et al., 2004). In addition to endocytosis of small vesicles, stimulation triggers bulk membrane retrieval, resulting in large vacuoles in the bipolar terminal (Holt et al., 2003; Paillart et al., 2003).

How direct is the vesicle cycle in the cone synapse, which unlike conventional synapses, tonically release transmitter? Is there bulk membrane retrieval or recycling through endosomes? Is there a large pool of immobilized reserve vesicles? Or, does the cone synapse

*Correspondence: rhkramer@berkeley.edu

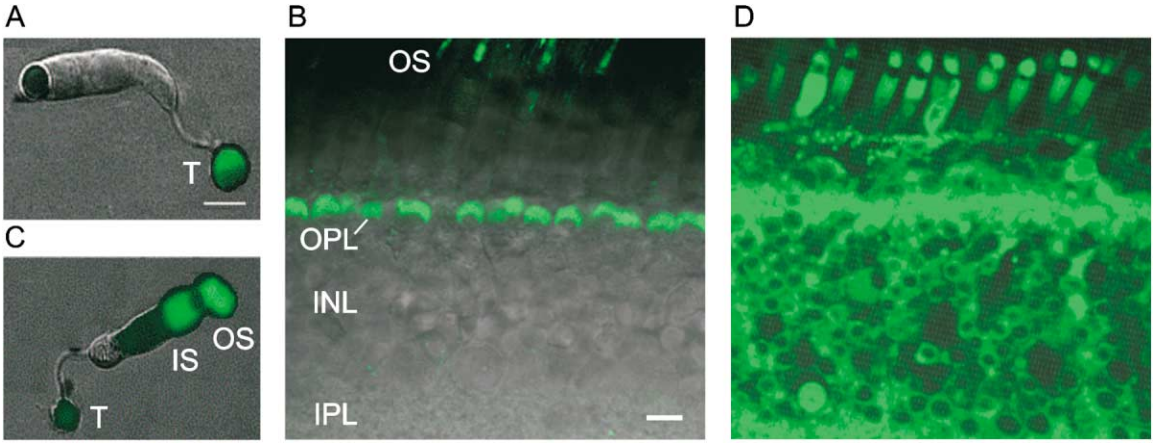

Figure 1. Specific Uptake of FM1-43 into Cone Terminals Is Achieved by Loading the Retina before Dissociation

(A) Single cone photoreceptor, loaded with FM1-43 prior to dissociation from the retina. Transmitted light and fluorescence images are overlaid. FM1-43 fluorescence is shown in green. T, synaptic terminal.

(B) Single cone loaded with FM1-43 following dissociation. IS, inner segment; OS, outer segment.

(C) Retinal slice, retina was loaded with FM1-43 prior to slicing. The position of the cone OS, outer plexiform layer (OPL), inner nuclear layer (INL), and inner plexiform layer (IPL) are indicated.

(D) Retinal slice, loaded with FM1-43 after slicing.

Scale bars, 10 μm.

support continuous release by employing a simpler vesicle cycle without these detours? At other synapses, the fluorescent styryl dye FM1-43 has been used to explore the vesicle cycle (for review, see Cochilla et al., 1999; Ryan, 2001). After staining the plasma membrane, the dye is internalized during endocytosis and can subsequently be released during exocytosis. However, FM1-43 can be taken up by other mechanisms into nonsynaptic portions of dissociated neurons (Rouze and Schwartz, 1998; Meyers et al., 2003), preventing its effective use in photoreceptor synapses. We find that when the dye is applied to the *intact* retina under conditions that stimulate continuous release, labeling is selective for synaptic terminals. Anole lizards have a cone-only retina, so in this preparation, labeling in the outer plexiform (OPL) is specific to cone terminals. Using this preparation and FM1-43 we explore the vesicle cycle of cones.

Results

Specific FM1-43 Labeling of Cone Terminals Requires Intact Tissue

We have optimized a procedure to specifically load FM1-43 into synaptic vesicles of cone terminals in the OPL. The intact dark-adapted lizard retina was incubated in normal saline in the dark with 45 μM dye for 15 min. To prevent exocytosis, which would unload the dye, the retina was then transferred to a Ca^{2+}-free solution containing EGTA. This solution also included Advasep-7, a cyclodextran that helps remove FM1-43 from surface membranes (Kay et al., 1999). FM1-43 labeling was then examined in individual dissociated cones (Figure 1A) and retinal slices (Figure 1B).

In preloaded dissociated cones (Figure 1A), intense FM1-43 fluorescence is apparent in the terminals but not in inner segments. In slices (Figure 1B), there was strong labeling in rows of cone terminals in the outer plexiform later (OPL) and in some cone outer segments, finely speckled labeling in the inner plexifom layer (IPL), but almost no labeling in cone inner segments or the inner nuclear layer (INL). Similar OPL-specific labeling was seen when FM1-43 was added to intact retina from tiger salamander, *Xenopus* frogs, goldfish, and rabbit (not shown). Both rod and cone terminals were labeled in these preparations, with little labeling of photoreceptor inner segments or the INL. Hence, by using intact retina, followed by a wash with Advasep-7, we have discovered a generally applicable method for synapse-specific loading of FM1-43 in retinal photoreceptors.

When FM1-43 was applied after retinal dissociation (Figure 1C) or slicing (Figure 1D), the labeling was not specific to terminals. The isolated cone showed labeling in all regions and was brightest in the inner segment (Figure 1C). Slices showed labeling in all layers, obscuring clear visualization of cone terminals in the OPL (Figure 1D). This extrasynaptic labeling after dissociation or slicing occurred in the absence of extracellular Ca^{2+}. Hence, uptake of FM1-43 is synapse specific when dye is added to intact retina but not when it is added after perturbing the retina by slicing or cell dissociation. Dye uptake into extrasynaptic regions after perturbation possibly occurs through membrane resealing mechanisms that involve exocytosis and endocytosis (McNeil and Terasaki, 2001) or through activation of ion channels that are permeable to FM1-43 (Meyers et al., 2003).

Loading and Unloading Are Ca^{2+} Dependent

To assess whether FM1-43 loading is Ca^{2+} dependent, FM1-43 was added to intact retina in saline containing either 1.5 mM Ca^{2+} or zero Ca^{2+} plus 1 mM EGTA (0 Ca^{2+}/EGTA). A strong band of labeling appeared within the OPL when FM1-43 was added in the presence but not in the absence of Ca^{2+} (Figure 2A). In three experiments with Ca^{2+}-containing saline, there was much

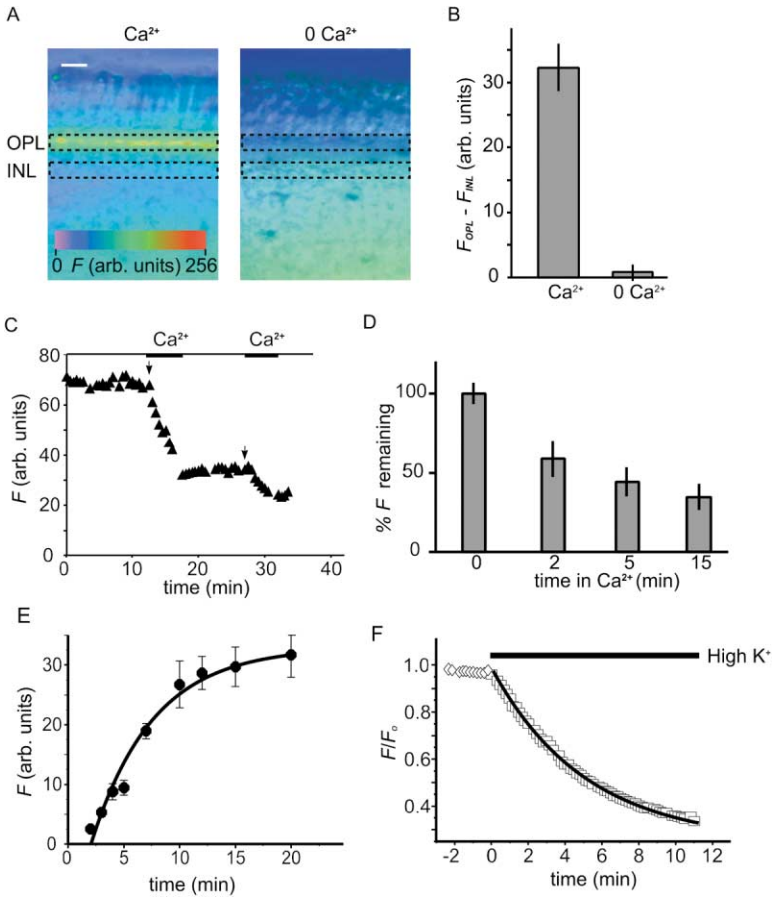

Figure 2. Loading and Unloading of FM1-43 Is Ca^{2+} Dependent

(A) Pseudocolor images of slices taken from retina preloaded with FM1-43 in the presence or absence of Ca^{2+}. Dashed boxes indicate OPL and INL regions used for analysis of fluorescence intensity, *F*. Scale bar, 20 μm.

(B) OPL fluorescence, F_{OPL}, following Ca^{2+}-dependent and Ca^{2+}-independent loading of FM1-43. To compensate for differences in background loading, the fluorescence of a region of the IPL was subtracted ($F_{OPL} - F_{IPL}$).

(C) A single slice from retina preloaded with FM1-43 was imaged every 30 s in high K^+, Ca^{2+}-free solution and 1.5 mM Ca^{2+} was applied as indicated. Fluorescence measurements across the OPL are plotted against time.

(D) Average loss of fluorescence from retina preloaded with FM1-43 after different times in high K^+/Ca^{2+} solutions (n = 3–5 slices).

(E) Kinetics of FM1-43 loading in Ca^{2+}/high K^+ saline. Fluorescence measurements were taken from the OPL of retina that were loaded for indicated times. Continuous line is a single exponential fit with $\tau = 332$ s.

(F) Kinetics of FM1-43 unloading in Ca^{2+}/high K^+ saline. Cone terminals in preloaded retina were visualized in retina slices, and loss of fluorescence was monitored at 10 s intervals. Continuous line is a single exponential fit with $\tau = 345$ s.

greater labeling intensity in this region of the OPL compared to a region of the same size in the INL, whereas in Ca^{2+}-free saline, there was no difference in OPL versus INL labeling (Figure 2B). Hence, FM1-43 loading into cone terminals is Ca^{2+} dependent.

To assess whether *un*loading of FM1-43 is also Ca^{2+} dependent, retinas were loaded and sliced and then exposed to saline containing high K^+ (50 mM) to depolarize cones and open voltage-gated Ca^{2+} channels. In an individual slice (Figure 2C), FM1-43 release could repeatedly be started by exposure to Ca^{2+}/high K^+ saline and stopped by exposure to 0 Ca^{2+}/EGTA. Analysis of FM1-43 release from many slices is shown in Figure 2D. All slices were incubated for a total period of 15 min and exposed for various periods of time to Ca^{2+}/high K^+ saline. Dye unloads progressively with increasing time in Ca^{2+}, with more than half unloading within 5 min. Hence, unloading of FM1-43 is Ca^{2+} dependent.

To learn more about the kinetics of endocytosis and exocytosis, we carefully examined the time course of FM1-43 loading and unloading (Figures 2E and 2F). To measure the kinetics of loading, intact retinas were exposed to dye in Ca^{2+}/high K^+ saline for a variable time (2–20 min) before washing with 0 Ca^{2+}/EGTA, slicing, and analyzing fluorescence in cone terminals. Data from 40 retinas (n = 3–6 per time point) showed that dye accumulation could be fit with a single exponential time course ($\tau = 332$ s) that reached steady state within about 10 min (Figure 2E). To measure the rate of unloading, slices of retina containing FM1-43-loaded terminals were exposed to Ca^{2+}/high K^+ saline, and the decline in fluorescence was measured at 10 s intervals (Figure 2F). These experiments showed that unloading also occurs over a single exponential time course ($\tau = 345$ s; n = 6). Hence, loading and unloading occur over a nearly identical time course, consistent with the idea that endocytosis and exocytosis are closely linked in photoreceptor terminals (Rieke and Schwartz, 1996).

Loaded FM1-43 Is Restricted to Synaptic Vesicles

Electron micrographs of thin (90 nm) sections showed the cone terminals to be densely packed with small synaptic vesicles throughout the terminal (Figure 3A). The terminals were roughly hemispherical with an average diameter of 6 μm, so we estimate from the number of vesicles in a single section that a terminal contains about 250,000 synaptic vesicles. Larger membranous structures (endosomes or cisternae) were absent. Synaptic ribbons were also seen at characteristic triad junctions with horizontal and bipolar cell dendrites, and there were also a few mitochondria.

FM1-43 inserts into plasma membrane and becomes internalized upon endocytosis of vesicles (Betz et al., 1992). However, FM1-43 can also enter some cells through ion channels, including the vanilloid receptor (TRPV1) and a purinergic receptor ($P2X_2$) (Meyers et al., 2003). Hence, under certain conditions, FM1-43 loading in retinal bipolar cells (Rouze and Schwartz, 1998) and

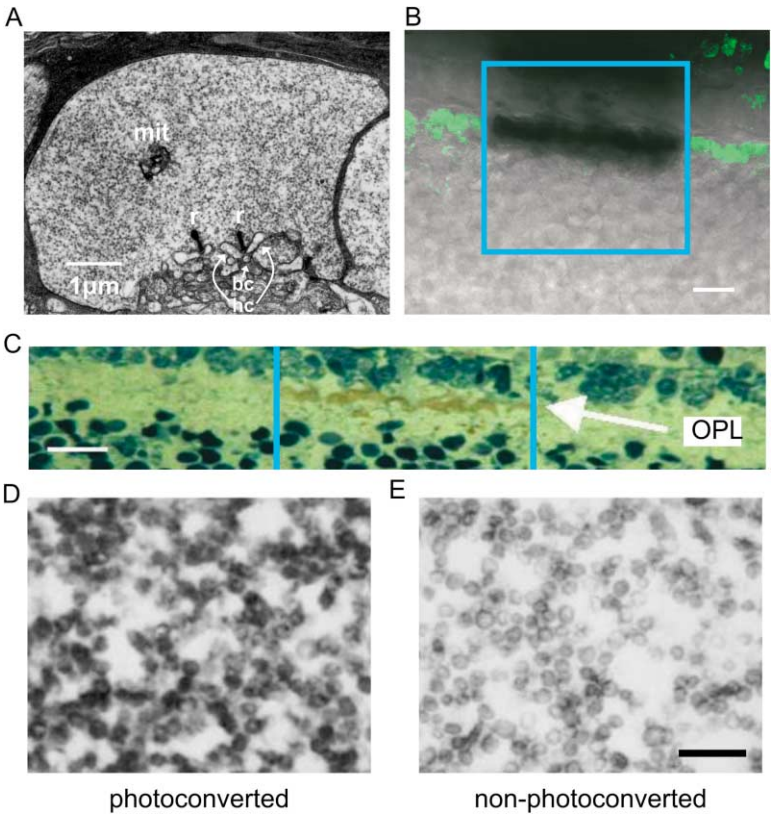

Figure 3. AM1-43 Is Localized to Synaptic Vesicles

(A) Electron micrograph of a lizard cone terminal filed with thousands of synaptic vesicles dispersed throughout. Also shown are synaptic ribbons (r), postsynaptic dendrites from horizontal and bipolar cells (hc and bc), and mitochondria (mit).

(B) Photobleaching of AM1-43 in the presence of DAB. The blue rectangle indicates the region centered on the OPL that was exposed to photobleaching laser light. Fluorescence and transmitted light images are overlaid to show AM1-43 fluorescence (green) and DAB reaction product (black) following photoconversion. Scale bar, 10 μm.

(C) Semithin section of a slice photoconverted as in (B). The blue rectangle indicates the photobleached region. DAB reaction product in cone terminals appears brown. The tissue was counterstained with Toluidine blue. Scale bar, 25 μm.

(D and E) Electron micrographs of an AM1-43 photoconverted (D) and control (E) cone terminal. Dense DAB reaction product is localized to synaptic vesicles in (D). Scale bar, 250 nm.

cochlear hair cells (Meyers et al., 2003) does not require extracellular Ca^{2+} and is not readily unloaded by promoting Ca^{2+} entry. Since some TRP channels are activated by Ca^{2+} (Launay et al., 2002), it seemed possible that such channels could contribute to Ca^{2+}-dependent uptake of FM1-43 in cone terminals. To test whether loading in cone terminals results exclusively from endocytosis, we used AM1-43, a structural analog of FM1-43 that can be crosslinked to proteins by fixation with glutaraldehyde. Intense illumination of AM1-43, in the presence of diaminobenzidine (DAB), results in "photoconversion" of the DAB to form an electron-dense reaction product that is visible with electron microscopy (EM) (Henkel et al., 1996a; Harata et al., 2001). Figure 3B shows a fluorescence image of a slice with AM1-43-loaded terminals that had been photobleached by prolonged illumination with strong 488 nm light. Transmitted light images from this slice show the brown reaction product localized in cone terminals (Figure 3C). EM images from photoconverted (Figure 3C) and control regions (Figure 3D) of the slice show that a large proportion (>80%) of synaptic vesicles in the photoconverted region were filled with electron-dense material, whereas in the control region, <1% of the vesicles were electron dense. Similar results were obtained in three experiments. About 50% of photoconverted vesicles had electron-dense "coats," suggesting a role for clathrin in endocytosis (Brodin et al., 2000; Slepnev and De Camilli, 2000). Notably, photoconversion did not raise the background density of cytoplasm, suggesting that AM1-43 was restricted to the lumen of vesicles. Hence, dye loading of cone terminals occurs specifically through endocytosis of vesicles.

Movement of Endocytosed Vesicles

Where do vesicles go after endocytosis in cone terminals? To answer this question, cone terminals in intact retina were loaded with FM1-43 in the dark. The retina was then washed with Advasep-7, to remove dye from surface membranes, plus 0 Ca^{2+}/EGTA, to prevent unloading. Then, in the continued presence of 0 Ca^{2+}/EGTA, we applied FM4-64 to selectively stain surface membranes. FM4-64 is chemically similar to FM1-43, but it has a different emission spectrum, allowing labeling by the two dyes to be distinguished. Thus, green FM1-43 fluorescence appeared in the interior of cone terminals (Figure 4A) with red FM4-64 on the surface membranes of cone terminals and other cells in the vicinity (Figure 4B).

Superimposing the two images (Figure 4C) shows FM1-43 entirely filling the cone terminal, suggesting that endocytosed vesicles are not restricted to specific regions and that no additional structures external to the cone terminal are labeled with FM1-43. A density profile taken through a terminal (Figure 4D) shows that Ca^{2+}-dependent labeling with FM1-43 and Ca^{2+}-independent labeling with FM4-64 show no overlap except within 1 μm of the membrane, near the limit of our spatial resolution. Hence endocytosed vesicles disperse throughout cone terminals, and these are the only structures in the OPL that incorporate appreciable amounts of FM1-43.

How rapidly do endocytosed vesicles disperse? To address this, we loaded with AM1-43 in the dark, washing with Advasep-7 and 0 Ca^{2+}/EGTA, and then fixed with glutaraldehyde. Fluorescence distributed nearly evenly through the terminal, either with a 2 min or 15 min loading period (Figures 5A and 5B). The normalized density profiles in Figure 5C show that, even though

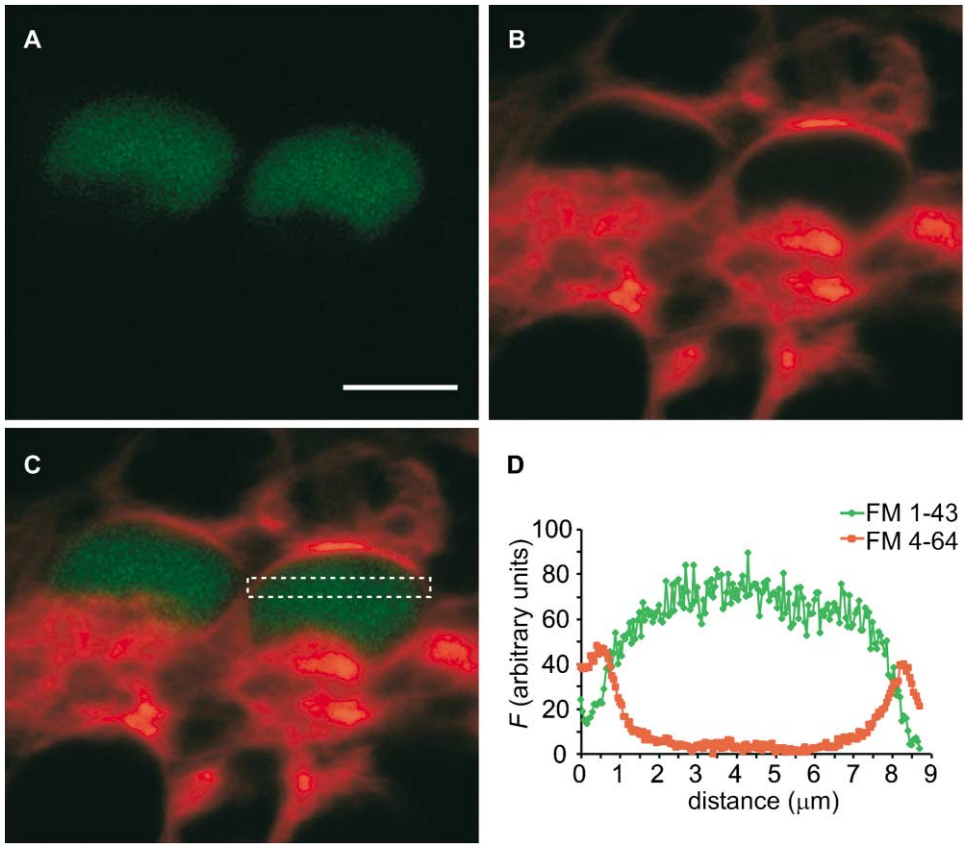

Figure 4. FM1-43 Fills the Entire Cone Terminal and No Other Structures in the OPL

(A) Confocal image of two cone terminals in a slice previously loaded with green FM1-43 with Ca^{2+} and then placed in red FM4-64 without Ca^{2+}. A 500–550 nm emission filter was used to pass only the FM1-43 fluorescence. Scale bar, 5 μm.

(B) The same region imaged through a 650 LP filter to pass only FM4-64 fluorescence. Gain settings were previously adjusted to remove bleedthrough of FM1-43 fluorescence (about 20% of the total signal).

(C) Overlay of images in (A) and (B), showing localization of the two dyes. Green labeling is in synaptic vesicles inside the terminals and red labeling is on surface membranes.

(D) Average fluorescence measured across one terminal, showing the intensity profile of both dyes. The region used for analysis is indicated in (C) (white dotted rectangle).

less total fluorescence is present, terminals loaded for ~2 min show the same fluorescence profile as terminals loaded for 15 min.

After dispersal, do labeled vesicles remain mobile? To address this question, loaded terminals were exposed to Ca^{2+}/high K^+ saline previously. Fluorescence remained nearly uniform across the terminal, both after a short 2 min unloading period (Figure 5D) and a long 15 min unloading period (Figure 5E). Again, a density profile through the terminal shows that the distribution of fluorescence remains remarkably similar both at the beginning and the end of the unloading period (Figure 5F). Hence, during unloading, labeled vesicles redistribute rapidly and are drained from the entire terminal, leaving no local areas devoid of vesicles.

To quantify vesicle mobility in cone terminals, we used Fluorescence Recovery After Photobleaching (FRAP) (Figure 6) in FM1-43-loaded terminals where vesicle cycling had been stopped with 0 Ca^{2+}/EGTA. Using a confocal scanning microscope, a small area (2 μm^2) in the center of a cone terminal was scanned with an Argon laser (488 nm) at full power for about 1.5 s. This bleached the FM1-43 such that vesicles within the region were no longer fluorescent (Figure 6A). Over time, the fluorescence within the bleached region recovered and fluorescence in the remainder of the terminal decreased as vesicles redistributed within the terminal. In control experiments, application of high K^+/Ca^{2+} saline was effective in unloading the FM1-43 that remained after local photobleaching, indicating that the procedure had not functionally damaged the terminal. Fluorescence intensity profiles across the terminal including the bleached region show how the fluorescence has redistributed at different times after the bleach (Figure 6B). The mobility of vesicles in the terminal can be assessed by comparing the recovery of fluorescence in the bleached region to the fluorescence across the whole terminal at each time point. The fluorescence recovery can be fitted to a biexponential function with time constants of ~2 s and 9 s (Figure 6C). However, recovery is incomplete, such that even after recovery reaches steady state (25 s) the ratio of fluorescence in the bleached to unbleached regions is 87% ± 2% (n = 10). This suggests that about 87% of vesicles are sufficiently mobile to exchange between

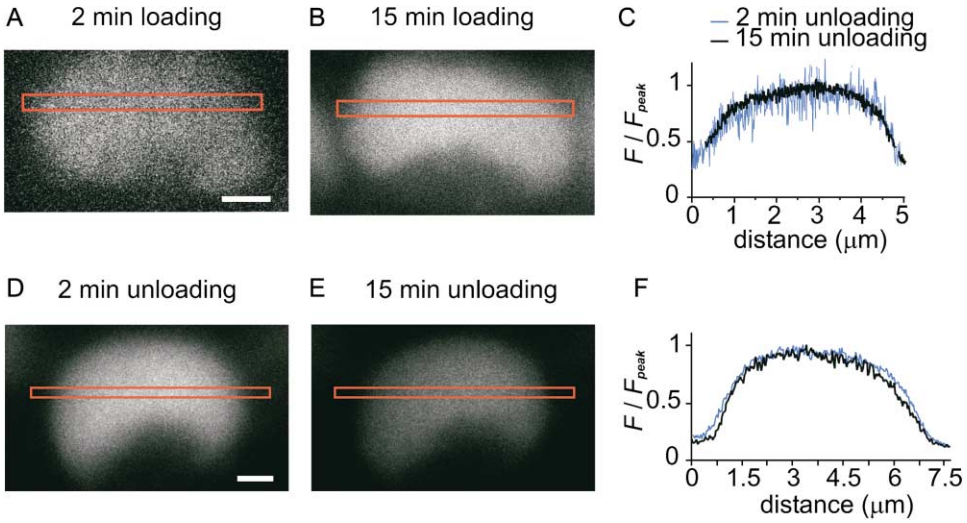

Figure 5. Vesicles Disperse Rapidly during FM1-43 Loading and Remain Evenly Dispersed during Unloading

(A and B) Vesicles disperse evenly and rapidly during loading. FM1-43 fluorescence in terminals following a 2 min (A) or 15 min (B) load with AM1-43. Slices were fixed with glutaraldehyde immediately after loading to prevent unloading during image acquisition.

(C) Very similar fluorescence profiles across the terminals loaded for 2 and 15 min. Average fluorescence, F, was normalized to peak average fluorescence, F_{peak}. Analysis regions are indicated in (A) and (B) (red rectangles).

(D and E) Vesicles remain evenly dispersed during unloading. Retina was preloaded with FM1-43 for 15 min and then unloaded in high K^+ solution for 2 (D) or 15 min (E).

(F) Very similar fluorescence profiles across the terminals unloaded for 2 and 15 min.

Scale bars, 1 μm.

the unbleached and bleached region (the mobile fraction). This stands in stark contrast to the neuromuscular junction, where FRAP measurements have shown that little recovery occurs even 1 hr after FM1-43 photobleaching, indicating that vesicles are immobile (Henkel et al., 1996b).

The position of the bleached region within the terminal did not substantially affect the rate or extent of FRAP. This applied even to areas at the base of the terminal that should contain synaptic ribbons. However, differences in the mobility of free vesicles and those residing on ribbons may be difficult to resolve considering that our EM evidence shows that less than 1% of vesicles reside on ribbons.

Further analysis of the FRAP results provides an estimate of the diffusion coefficient (D) for mobile synaptic vesicles. To determine the rate of vesicle movement, we fitted the FRAP time course to the solution of the diffusion equation based on a fit of the photobleach profile with a Fourier expansion (Berk et al., 1993). This solution takes the form of an infinite series of exponentials, but the first two terms are sufficient to describe the FRAP time course. Hence, FRAP data were fitted with a double exponential function. By using the time constant for the slowest component (9 s), which was best resolved with our data acquisition, it was possible to estimate D for synaptic vesicles within photoreceptor terminals. This yielded a value of 1.1×10^{-9} cm^2/s. Because $D = (distance)^2/6(time)$ for diffusion in three dimensions, a synaptic vesicle will on average move 1 μm in 1.5 s.

Is the mobility of vesicles modulated by intracellular messengers that regulate the release rate? We tested whether elevated intracellular Ca^{2+} influences FRAP by applying a Ca^{2+} ionophore. Adding 5 μM ionomycin in conjunction with normal (1.5 mM) external Ca^{2+} increased internal Ca^{2+} from ~50 nM to ~0.5 μM within 2 min (Rea et al., unpublished data), but had no effect on the mobile fraction of vesicles ($n = 27$) (Figure 6D). Neither adding 1 μM forskolin to activate adenylate cyclase and trigger cAMP production ($n = 26$) nor adding 50 μM 8-Br-cAMP ($n = 13$) affected vesicle mobility. Hence, vesicle mobility does not appear to be regulated by intracellular Ca^{2+} or cAMP. Treatment with 1 μM okadaic acid (OA), a protein phosphatase inhibitor, decreased the percentage of mobile vesicles to 74% ± 11% ($n = 8$), slightly less than control ($p = 0.1$). Okadaic acid slows the spread of FM1-43 fluorescence in bipolar cell terminals but has no effect on the kinetics of release (Guatimosim et al., 2002). Together with these results, our findings suggest that protein phosphorylation may play some role in regulating vesicle mobility, but it is unlikely to have a large impact on vesicles cycling at ribbon synapses.

Endocytosed Vesicles Retain Their Integrity Throughout the Vesicle Cycle

To determine whether endocytosed vesicles retain their identity or whether they fuse with other vesicles or endosomes in cone terminals, we compared simultaneous versus sequential loading of FM1-43 and FM4-64. The absorbance spectrum of FM4-64 overlaps with the emission spectrum of FM1-43, so when they are mixed together, FM4-64 can quench FM1-43 fluorescence (Rouze and Schwartz, 1998). To test whether vesicular membranes intermingle during the vesicle cycle, we used the four protocols illustrated in Figure 7. First, cone terminals were loaded for 15 min in the dark with 45 μM

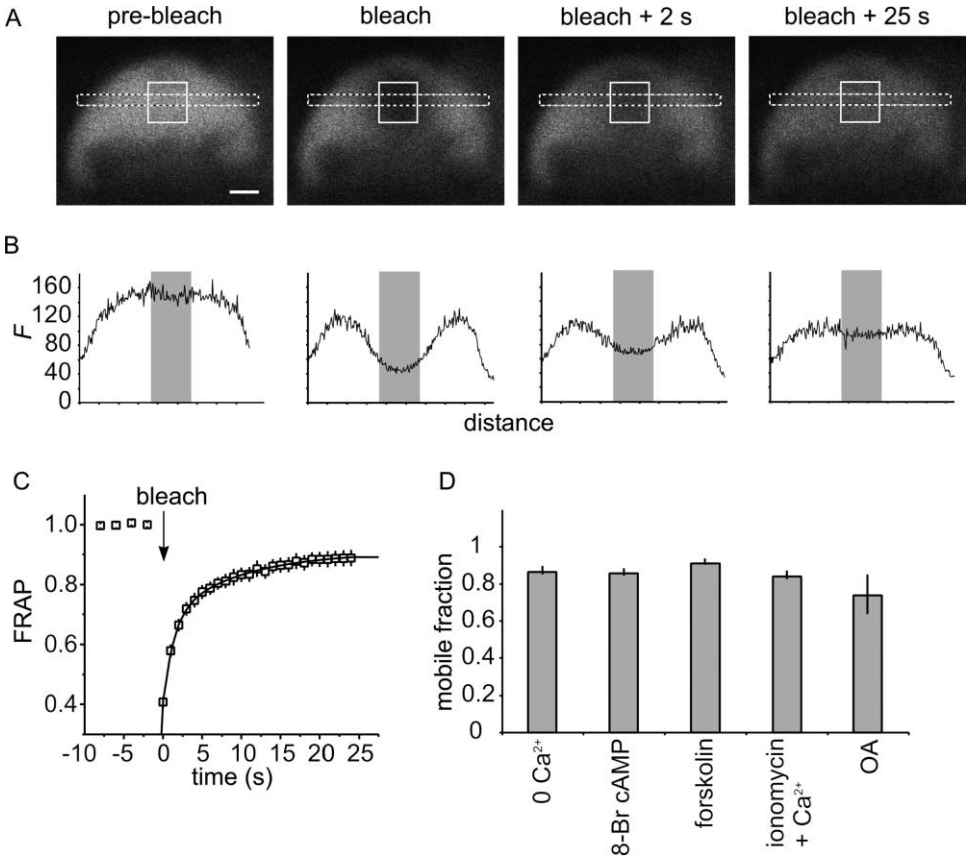

Figure 6. FRAP Experiments Reveal Rapid Vesicle Mobility

(A) Series of images taken from a single terminal in a slice preloaded with FM1-43, showing fluorescence before and after photobleaching of a 2 μm^2 region (white square). Confocal section thickness was 1.7 μm. Scale bar, 1 μm.

(B) Profiles of average fluorescence, *F*, across the terminal. The white dotted rectangles in (A) indicate the profile region, and the shaded rectangle indicates the bleached region.

(C) Time course of FRAP for terminals in Ca^{2+}-free saline. Photobleaching at time = 0 s. Average fluorescence in the bleached region was divided by average fluorescence over the whole terminal for each image. These ratios were then normalized to the ratio before the bleach (time = −2 s). Continuous line shows fit to a double exponential function with time constants of 1.4 and 9 s.

(D) The size of the mobile fraction of vesicles is unaffected by intracellular messengers. The mobile fraction was estimated from the percentage of FRAP measured at 25 s after bleach in slices incubated for 30 min with 0 Ca^{2+} saline alone or saline also containing 50 μM 8-Br cAMP, 1 μM forskolin, 5 μM ionomycin (with 1.5 mM Ca^{2+} for 15 min), or 1 μM OA. Data are from three to five experiments in each case.

FM1-43 alone (protocol 1). This served as a reference for the next experiment, in which the same concentration of FM1-43 was loaded for 15 min, but this time in the presence of 90 μM FM4-64 (protocol 2). Since FM1-43 and FM4-64 should label the same vesicles, protocol 2 should establish the maximal amount of quenching when FM1-43 and FM4-64 are maximally intermixed in the same internalized membranes. Third, we loaded 45 μM FM1-43 for 15 min and then added 90 μM FM4-64 for 5 min (protocol 3). If the vesicles loaded with FM1-43 coalesce with vesicles containing FM4-64, there should be some quenching. Finally, FM1-43 was loaded for 15 min, followed by 5 min with neither dye (protocol 4). This controlled for the unloading of FM1-43 that would occur during the 5 min of loading FM4-64 in protocol 3.

Figure 7 (top) compares the results of protocols 1 and 2. Simultaneous loading with FM1-43 and FM4-64 for 15 min results in a 69% ± 4% reduction in the FM1-43 fluorescence (n = 4), suggesting substantial quenching. To control for the possibility that the extra FM4-64 added in protocol 2 reduced FM1-43 fluorescence not by quenching but by saturating the uptake of the dye, we examined terminals loaded with 135 μM FM1-43 alone for 15 min. The fluorescence signal in these terminals was 1.4 ± 0.02 times larger than terminals loaded with 45 μM FM1-43 (n = 6), a significant increase ($p < 0.01$). Hence, dye uptake was not saturating in these experiments.

Figure 7 (bottom) compares the results of protocols 3 and 4. Loading sequentially with FM1-43 for 15 min and then FM4-64 for 5 min results in a FM1-43 produced fluorescence that was not significantly different (86% ± 15%) from that obtained by loading with FM1-43 for 15 min followed by 5 min unloading (n = 3). Hence, sequential loading does not allow quenching of FM1-43 by FM4-64, suggesting that vesicles loaded separately with one dye or the other do not intermix.

It is possible that, rather than fusing with an internal endosome after fission from the plasma membrane,

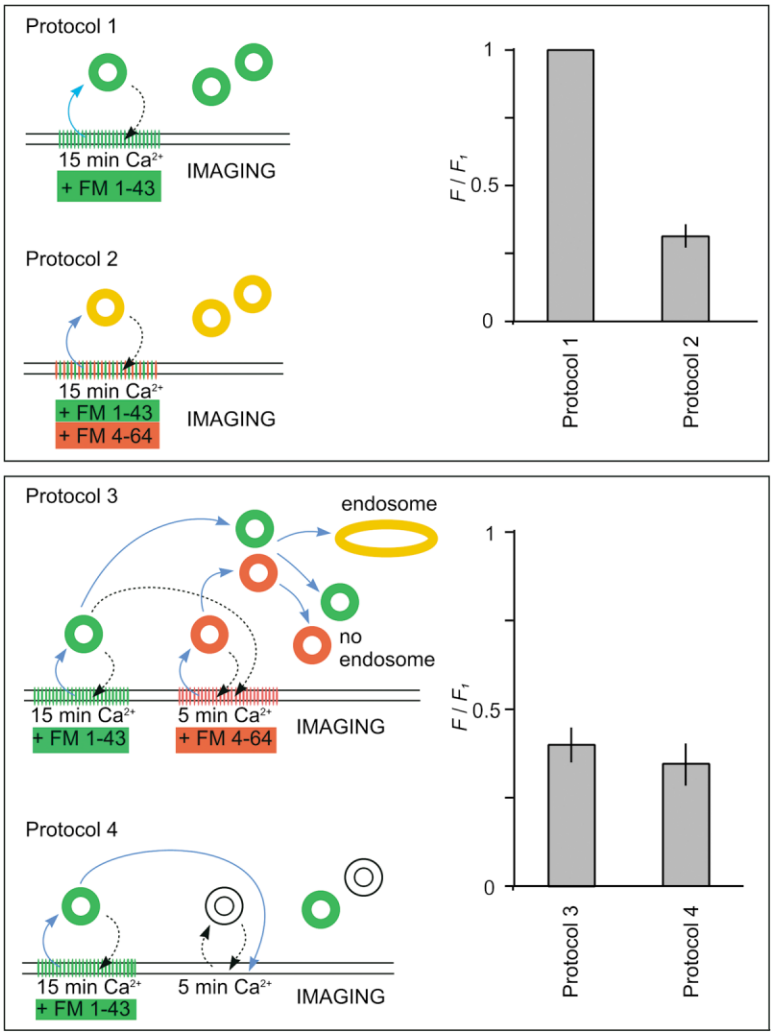

Figure 7. Vesicles Retain Their Integrity Throughout the Vesicle Cycle

Retinas were loaded with four different protocols. Protocol 1 (independent loading): FM1-43 was loaded for 15 min in the presence of Ca^{2+} and then transferred to Ca^{2+}-free solution for imaging. Protocol 2 (simultaneous loading): FM1-43 and FM4-64 were mixed together and then loaded for 15 min in the presence of Ca^{2+}. Orange color indicates mixing of the two dyes in the vesicle membrane. Protocol 3 (sequential loading): retina were loaded with FM1-43 for 15 min, washed in Ca^{2+}-free saline, and then loaded further with FM4-64 for 5 min. Diagram indicates the possibility that FM1-43 and FM4-64 may mix, if vesicles individually containing one dye fuse with endosomes, eventually producing vesicles containing both dyes (orange). Note that some FM1-43 vesicles unload during the second loading step. Protocol 4: FM1-43 was loaded for 15 min and then unloaded in Ca^{2+} for 5 min to estimate the extent of FM1-43 unloading in the second step of protocol 3. Bar charts show the average FM1-43 fluorescence, F, measured from terminals under each condition, normalized to the fluorescence of terminals loaded by Protocol 1, F_1.

large vesicles are endocytosed and then subdivide to form smaller synaptic vesicles. Evidence for endocytosis of ferritin into large structures in retinal bipolar cells has been obtained from EM observations (Paillart et al., 2003) and using a tetrarhodamine-labeled 40 kDa dextran (TAMRA-40K-DEX) which is also preferentially taken up into large vacuoles (Holt et al., 2003). EM studies on chick photoreceptors also show that extracellular horseradish peroxidase tracer appears in large vacuoles in some photoreceptor terminals in a dark-dependent manner (Cooper and McLaughlin, 1983). To test whether large vacuoles form in lizard cone terminals, we incubated slices in Ca^{2+}/high K^+ saline with TAMRA-40K-DEX for 15 min ($n = 2$) or 30 min ($n = 2$). Subsequent examination of cone terminals with confocal microscopy showed TAMRA-40K-DEX internalization in 26% (15 min) and 18% (30 min) of terminals as compared to >95% when terminals were loaded with FM1-43. Terminals that did take up TAMRA-40K-DEX showed diffuse rather than punctate labeling, suggesting uptake into relatively small structures. Examination of EM images also failed to show large vacuoles in any of 20 cone terminals examined. Therefore, it is unlikely that bulk membrane retrieval is a part of the vesicle cycle in lizard cones, even when they have been strongly depolarized with Ca^{2+}/high K^+ saline.

Discussion

Activity-Dependent Loading of FM1-43 into Cone Terminals

FM1-43 is an important tool for studying presynaptic function and membrane trafficking in neurons and other cell types (for review, see Cochilla et al., 1999; Ryan, 2001). It has been particularly useful for exploring synaptic function in ribbon synapses of retinal bipolar cells (Lagnado et al., 1996; Rouze and Schwartz, 1998; Mack et al., 2000; Zenisek et al., 2002; Guatimosim et al., 2002). However, Ca^{2+}-independent extrasynaptic labeling has precluded its use in dissociated photoreceptors. We have shown that simply by applying the dye while the retina is still intact and then washing with Advasep-7, photoreceptor terminals are loaded selectively without labeling neighboring structures such as horizontal and bipolar cell terminals. Loading and unloading are Ca^{2+} dependent, and electron microscopy shows that the dye is located specifically in synaptic vesicles. Thus, even though FM1-43 can enter cells through routes other than

endocytosis (Rouze and Schwartz, 1998; Meyers et al., 2003), dye uptake into cone terminals in intact retina occurs primarily through endocytosis of surface membrane.

The synapse-specific loading of FM1-43 has enabled us to explore the vesicle cycle in cones. Moreover, activity-dependent loading and unloading opens the opportunity to explore how light and other stimuli regulate transmitter release. Most of what we know about how release is regulated comes indirectly from recordings of postsynaptic responses from retinal bipolar and horizontal cells. However, these responses are determined not only by the rate of photoreceptor exocytosis but also by diffusion in the synaptic cleft, the rate of glutamate reuptake (Gaal et al., 1998), the properties of postsynaptic glutamate receptors, and the effects of electrical and/or chemical feedback from HCs onto cone terminals (Kamermans and Spekreijse, 1999). It was established long ago that cone terminals accumulate markers, such as horseradish peroxidase, in small vesicles in the dark (Ripps et al., 1976; Schacher et al., 1976; Schaeffer and Raviola, 1978). However, these experiments required long incubation times (hours) and labeling could not be observed in real time, but only after permeabilizing the tissue. FM1-43 allows direct measurement of how light affects cone exocytosis in real time (Rea et al., unpublished data). Moreover, measurements can be made not only on isolated cells but also on arrays of cone terminals in retinal slices or retinal flat mounts (Rea et al., unpublished data), allowing release to be evaluated as it occurs in the intact system. Even though the OPL contains horizontal, bipolar, and Müller glial cells along with photoreceptor terminals, the only structures exhibiting considerable membrane cycling in the dark, and therefore FM1-43 loading, are rod and cone terminals. Since anole lizards possess cones but no rods, we have discovered a way to understand synaptic information transfer in a defined synaptic layer of the CNS from a homogenous population of cells.

The Vesicle Cycle in Cones

Figure 8 shows our proposed sequence of events in the vesicle cycle. After fusion of synaptic vesicles with the membrane and release of the neurotransmitter glutamate (1), membrane is retrieved by endocytosis of small vesicles (2a). Unlike other synapses, endocytosis *does not* appear to involve bulk membrane retrieval (2b). Endocytosed vesicles diffuse from their site of origin throughout the terminal (3) and eventually encounter and bind to a synaptic ribbon (4a). Steps 4b and 4c illustrate events that are common in many synapses but are, at most, of minor significance to the vesicle cycle of cones. Only a small proportion of vesicles become tethered to the cytoskeleton (4b), and there is no evidence for vesicles fusing and intermingling their membranes with other vesicles in endosomes (4c). In contrast, the high mobility of synaptic vesicles is important for increasing the likelihood that vesicles will encounter and bind to a synaptic ribbon (4a). Vesicles then move along the synaptic ribbon, are primed for release, and dock to the plasma membrane (5). Elevated intracellular Ca^{2+} triggers fusion of docked synaptic vesicles (1), completing the cycle.

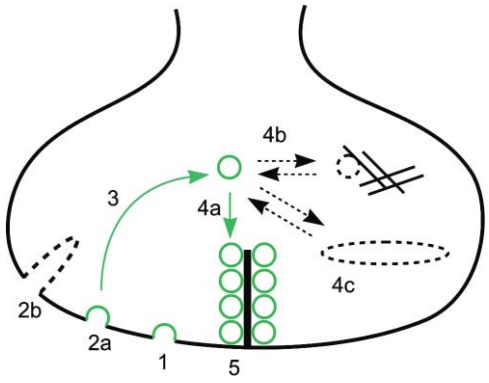

Figure 8. The Steps in the Vesicle Cycle of Cones

(1) Fusion of synaptic vesicles with the plasma membrane; (2a) retrieval by endocytosis of small vesicles; (3) dispersal of vesicles throughout the cone terminal; (4a) binding to a synaptic ribbon; (5) movement along the ribbon, priming, and docking to plasma membrane; (1) fusion of synaptic vesicles with the plasma membrane. Our evidence suggests that step 2b (bulk membrane retrieval), step 4b (immobilization of vesicles by tethering to the cytoskeleton), and step 4c (fusion with an intracellular endosome) are not usual parts of the vesicle cycle.

The vesicle cycle of cones does not seem to involve bulk membrane retrieval or an endosomal intermediate step. When endocytosed vesicles are retrieved from the plasma membrane, they must recoup important lipid and protein constituents needed for the next round of exocytosis. By avoiding the mixing of membrane constituents that could occur in vacuoles formed by bulk membrane retrieval or by fusing vesicles with an endosomal intermediate, cone terminals avoid the extra step of sorting and parsing out of these constituents as new vesicles are born. Perhaps conventional synapses with a large reserve pool can afford to side track at least some of their vesicles through an endosomal intermediate (Heuser and Reese, 1973; Ryan et al., 1996; Richards et al., 2000). However, even at these synapses there is evidence that many cycling vesicles retain their integrity and are reused (Ceccarelli et al., 1973; Murthy and Stevens, 1998) and that endosomes may only be important with intense stimulation (Richards et al., 2003). Most conventional synapses are remote from neuronal somata. These synapses might use an intermediate endosomal step in the vesicle cycle as a quality control mechanism for extensively reused synaptic vesicle proteins. Perhaps the relatively close proximity of cone terminals to inner segments makes such a step unnecessary.

Our diagram of the vesicle cycle does not include much shorter cycles that might occur, including multiple rounds of kiss-and-run exocytosis, the shortest vesicle cycle possible. Recent studies on hippocampal synapses in culture suggest that many fusion events are of the kiss-and-run variety (Aravanis et al., 2003; Gandhi and Stevens, 2003), characterized by repeated transient and incomplete fusion of vesicles with the plasma membrane. FM1-43 is, at best, incompletely released during these events, because fusion pore openings are too brief to allow rapid release of the dye, which dissociates slowly from membranes. However, FM2-10 is more hydrophilic, dissociates more rapidly, and therefore is fully

released even during kiss-and-run exocytosis (Klingauf et al., 1998). We find no difference in the unloading rate of FM1-43 and FM2-10 during application of high K^+/Ca^{2+} saline (Rea et al., unpublished data). Therefore, the vesicle cycling revealed by FM1-43 may account for nearly all of the transmitter release from the cone terminal, without involving kiss-and-run exocytosis.

Synaptic Vesicle Mobility

FM1-43-containing vesicles disperse evenly through cone terminals within 2 min after uptake. Even many minutes after dye uptake, vesicles remain mobile, suggesting that most vesicles do not become tethered to the cytoskeleton. The percentage of vesicles that are mobile and the diffusion rate of mobile vesicles are both unaffected by elevating Ca^{2+}. This is in contrast to neuromuscular and hippocampal synapses, where the mobility of vesicles is highly restricted both before and during stimulation (Henkel et al., 1996b; Kraszewski et al., 1996). We have calculated the diffusion coefficient of synaptic vesicles in cones, which we measure as having an average diameter of about 50 nm (unpublished data). Assuming that the cytoplasmic viscosity and density of the cytoskeletal matrix in cone terminals are similar to those of fibroblasts, the measured diffusion coefficient of synaptic vesicles (0.11 $\mu m^2/s$) is similar to the rate that an inert particle of similar diameter (50 nm) would diffuse passively (0.15 $\mu m^2/s$) (Luby-Phelps et al., 1987). This suggests that synaptic vesicles in cones diffuse without binding to structures that could hinder their movement. Consistent with this, synaptic vesicles in cones appear to move randomly with no particular directionality, for example, toward release sites at the base of the terminal.

In bipolar cells, indirect measurements have suggested that peripheral vesicles are mobile, but central vesicles are not (Lagnado et al., 1996). However, a recent study using more direct measures of mobility suggests that most vesicles throughout the bipolar terminal are mobile and that this is also unaffected by raising intracellular Ca^{2+} (Holt et al., 2004). These features of vesicle mobility are qualitatively similar to those in cone terminals. Yet, vesicles move ten times more quickly in cone terminals than in bipolar terminals. Thus, mobility seems to correlate with the capacity for tonic release, with conventional phasic terminals having immobile vesicles, tonic cone terminals having maximally mobile vesicles, and phasic-tonic bipolar terminals having vesicles of intermediate mobility.

At nearly all synapses, synaptic vesicles are tethered to the cytoskeleton through the membrane-associated protein synapsin, which binds to actin (Hilfiker et al., 1999). Intracellular Ca^{2+} and cAMP, via CaMKII and PKA, respectively, can trigger the phosphorylation of synapsin, decreasing its affinity for actin. Synapsin phosphorylation, and consequently mobilization of tethered vesicles, is one of several Ca^{2+}- and cAMP-mediated events that have been implicated in modulation of secretion from presynaptic terminals. Remarkably, vertebrate rods and cones from nearly all species lack synapsin (Von Kreigstein et al., 1999; Morgans, 2000). This may account for the high mobility of synaptic vesicles in cones and may also help explain why Ca^{2+} and cAMP have no effect on mobility. Okadaic acid, a protein phosphatase inhibitor, slightly decreases vesicle mobility in cones, suggesting that there might be some other phosphoprotein that can regulate interactions between synaptic vesicles and other structures in the cytoplasm. However, it appears that the mobility of vesicles and presumably their delivery to synaptic ribbons is largely unregulated in cones. The average time required for a synaptic vesicle to traverse a 6 μm diameter cone terminal is seven times faster than the time constant of release (48 s versus 345 s), indicating that vesicle mobility is not rate limiting for release. Therefore, subsequent steps in the vesicle cycle, for example, movement along the ribbon, docking to the plasma membrane, or fusion itself, must be rate limiting for continuous release. Moreover, small changes in the size of the mobile fraction of vesicles or in the rate of their movement should have little effect on release from cones.

Most synaptic terminals, including those of retinal bipolar cells (Lagnado et al., 1996; von Gersdorff et al., 1996), contain a large reserve pool of synaptic vesicles that are relatively immobile and cannot easily be released. Strong and prolonged stimulation depletes the readily-releasable pool, resulting in depression of the rate of vesicle fusion and therefore synaptic transmission. With intense stimulation at phasic synapses, vesicles are mobilized from the reserve pool to help replenish the readily-releasable pool (Hilfiker et al., 1999; Zucker and Regehr, 2002). In contrast, our results suggest that there is almost no reserve pool in cones. About 87% of labeled vesicles remain mobile 1 hr after dye loading, the majority of vesicles in loaded terminals appear electron dense after photoconversion, and most of the loaded dye can be released upon depolarization with high K^+.

The lack of a reserve pool and the huge number of highly mobile vesicles insures that synaptic ribbons in cones remain fully charged with synaptic vesicles. This limits the extent of synaptic depression, even in the face of a high tonic release rate in the dark. Intense stimulation of cochlear hair cells, which also have tonic synapses, depletes the number of docked vesicles and vesicles in the cytoplasm, but to a lesser extent the number associated with ribbons (Lenzi et al., 2002). This suggests that ribbons have a relatively high affinity for vesicle binding. We propose that cytoplasmic vesicles are kept highly mobile to help keep ribbons saturated with vesicles. This should minimize fluctuations in the number of vesicles that are immediately available for release, allowing changes in Ca^{2+}-dependent exocytosis to accurately represent changes in illumination.

Experimental Procedures

Retinal Preparation and FM Loading

Anolis segrei lizards maintained on a 12:12 hr light:dark cycle were used for all experiments. The care and use of these animals was approved by the UC Berkeley Animal Care and Use Committee. Eyes were removed following decapitation and pithing, and dark-adapted on ice for 30 min in normal lizard saline (in mM: NaCl 149; KCl 4; $CaCl_2$ 1.5; $MgCl_2$ 1.5; HEPES 10; glucose 10; pH 7.5) before removal of the retina. Enucleation was carried out in normal saline in the dark under infrared light, using IR viewers attached to a dissecting microscope. The retina was separated manually from the retinal pigment epithelium (RPE) and loaded with dye (FM1-43, FM4-

64, or AM1-43) in normal saline for 15 min in the dark. Unless otherwise stated, loading was followed by washing in 0 Ca^{2+}/EGTA solution (same as normal saline, but with 1 mM EGTA substituted for 1.5 mM Ca^{2+}). FM or AM dyes were removed from external membranes by washing with 1 mM Advasep-7 (Kay et al., 1999) for 15 min. About 1/3 of the retina was cut from a position lateral to the optic nerve and fovea and prepared for imaging. For retinal slices, the piece of retina was flattened onto nitrocellulose paper with the photoreceptor side uppermost and cut into 300 μm thick slices using a tissue chopper. In experiments examining the distribution of dye at given time points of endocytosis, the tissue was fixed in 2.5% glutaraldehyde before slicing, within 2 min after dye loading. For dissociated cell preparations, the piece of retina was treated with 10 U/ml papain plus 1 mg/ml cysteine for 15 min, transferred to 10 mg/ml BSA for 2 min, and finally triturated gently five to ten times using a narrow glass pipette (0 Ca^{2+}/EGTA solution used for all three stages). A suspension of dissociated cones was then transferred onto a coverslip for imaging.

Imaging

Images were obtained with a Zeiss Axioplan 2 upright microscope and Zeiss 510 confocal system equipped with a 488 nm argon laser. Fluorescence was imaged with a 63× achroplan, 0.9 NA water-immersion objective. Additional magnification, time series, and photobleach protocols were controlled by Zeiss LSM acquisition software. For FRAP experiments, a 2 μm^2 region of the terminal was continually scanned five times at maximum laser power (total photobleach time 1.5 s). For examination of dye localization within a single terminal and for FRAP experiments, images were acquired with a spatial resolution of 33 pixels per micron and optical section thickness of 1.7 μm ($\sim$1 Airy unit). Scion Image software (Scion Corporation, Frederick, MD) was used for image analysis. FM1-43 (or AM1-43) and FM4-64 dyes were excited using the 488 nm laser line, and emitted light was collected through a 500-550BP or 650LP filter, respectively. In experiments examining FM4-64 fluorescence in double-loaded tissue, FM1-43 bleedthrough into the 650LP channel was first assessed by imaging a sample loaded with FM1-43 alone, and the gain settings then reduced to below the threshold for FM1-43 fluorescence. Variability among data is expressed as mean $\pm$ SEM. Student's t test was used to assess statistical significance at $p < 0.05$ unless stated otherwise.

Electron Microscopy

Slices were prepared from retina previously loaded with 45 μM AM1-43. Slices were then fixed in 2.5% glutaralydehyde in 0.1 M phosphate buffer (PBS) overnight at 4°C. After fixation, slices were washed in 100 mM glycine solution for 1 hr to reduce glutaraldehyde autofluorescence. Slices were then incubated in 1 mg/ml diaminobenzidine (DAB) solution (sonicated and filtered) in PBS at 21°C for 30 min, before exchanging for fresh DAB solution. Photoconversion of DAB was achieved using a confocal microscope by focusing high power, 488 nm light from an argon laser onto a 60 μm^2 region of the slice to include a row of AM1-43-loaded terminals for 8 min. Following photoconversion, the slice was trimmed to enable location of the photoconverted region and prepared for electron microscopy by dehydration and embedding as described previously (von Gersdorff et al., 1996).

Acknowledgments

We thank Sue Yeon Choi for help with TAMRA-40K-DEX experiments and Fred Lanni and Diek Wheeler for assistance with FRAP analysis. This work was supported by NIH grants to R.H.K. (EY12608), E.S.L. (NS 32385), and P.S. (EY08124) and a Fight for Sight grant (to R.H.K.). E.S.L. was a Miller Visiting Professor at UC Berkeley.

Received: September 24, 2003
Revised: January 23, 2004
Accepted: February 10, 2004
Published online: February 12, 2004

References

Aravanis, A.M., Pyle, J.L., and Tsien, R.W. (2003). Single synaptic vesicles fusing transiently and successively without loss of identity. Nature *423*, 643–647.

Ashmore, J.F., and Copenhagen, D.R. (1983). An analysis of transmission from cones to hyperpolarizing bipolar cells in the retina of the turtle. J. Physiol. *340*, 569–597.

Berk, D.A., Yuan, F., Leunig, M., and Jain, R.K. (1993). Fluorescence photobleaching with spatial Fourier analysis: measurement of diffusion in light-scattering media. Biophys. J. *65*, 2428–2436.

Betz, W.J., Mao, F., and Bewick, G.S. (1992). Activity-dependent fluorescent staining and destaining of living vertebrate motor nerve terminals. J. Neurosci. *12*, 363–375.

Brodin, L., Low, P., and Shupliakov, O. (2000). Sequential steps in clathrin-mediated synaptic vesicle endocytosis. Curr. Opin. Neurobiol. *10*, 312–320.

Ceccarelli, B., Hurlbut, W.P., and Mauro, A. (1973). Turnover of transmitter and synaptic vesicles and the frog neuromuscular junction. J. Cell Biol. *57*, 499–524.

Cochilla, A.J., Angleson, J.K., and Betz, W.J. (1999). Monitoring secretory membrane with FM1–43 fluorescence. Annu. Rev. Neurosci. *22*, 1–10.

Cooper, N.G., and McLaughlin, B.J. (1983). Tracer uptake by photoreceptor synaptic terminals. I. Dark-mediated effects. J. Ultrastruct. Res. *84*, 252–267.

Fuchs, P.A., Glowatzki, E., and Moser, T. (2003). The afferent synapse of cochlear hair cells. Curr. Opin. Neurobiol. *13*, 452–458.

Gaal, L., Roska, B., Picaud, S.A., Wu, S.M., Marc, R., and Werblin, F.S. (1998). Postsynaptic response kinetics are controlled by a glutamate transporter at cone photoreceptors. J. Neurophysiol. *79*, 190–196.

Gandhi, S.P., and Stevens, C.F. (2003). Three modes of synaptic vesicular recycling revealed by single-vesicle imaging. Nature *423*, 607–613.

Guatimosim, C., Hull, C., Von Gersdorff, H., and Prado, M.A. (2002). Okadaic acid disrupts synaptic vesicle trafficking in a ribbon-type synapse. J. Neurochem. *82*, 1047–1057.

Harata, N., Ryan, T.A., Smith, S.J., Buchanan, J., and Tsien, R.W. (2001). Visualizing recycling synaptic vesicles in hippocampal neurons by FM 1–43 photoconversion. Proc. Natl. Acad. Sci. USA *98*, 12748–12753.

Henkel, A.W., Lubke, J., and Betz, W.J. (1996a). FM1–43 dye ultrastructural localization in and release from frog motor nerve terminals. Proc. Natl. Acad. Sci. USA *93*, 1918–1923.

Henkel, A.W., Simpson, L.L., Ridge, R.M., and Betz, W.J. (1996b). Synaptic vesicle movements monitored by fluorescence recovery after photobleaching in nerve terminals stained with FM1–43. J. Neurosci. *16*, 3960–3967.

Heuser, J.E., and Reese, T.S. (1973). Evidence for recycling of synaptic vesicle membrane during transmitter release at the frog neuromuscular junction. J. Cell Biol. *57*, 315–344.

Hilfiker, S., Pieribone, V.A., Czernik, A.J., Kao, H.T., Augustine, G.J., and Greengard, P. (1999). Synapsins as regulators of neurotransmitter release. Philos. Trans. R. Soc. Lond. B Biol. Sci. *354*, 269–279.

Holt, M., Cooke, A., Wu, M.M., and Lagnado, L. (2003). Bulk membrane retrieval in the synaptic terminal of retinal bipolar cells. J. Neurosci. *23*, 1329–1339.

Holt, M., Cooke, A., Neef, A., and Lagnado, L. (2004). High mobility of vesicles supports continuous exocytosis at a ribbon synapse. Curr. Biol. *14*, 173–183.

Kamermans, M., and Spekreijse, H. (1999). The feedback pathway from horizontal cells to cones. A mini review with a look ahead. Vision Res. *39*, 2449–2468.

Kay, A.R., Alfonso, A., Alford, S., Cline, H.T., Holgado, A.M., Sakmann, B., Snitsarev, V.A., Stricker, T.P., Takahashi, M., and Wu, L.G. (1999). Imaging synaptic activity in intact brain and slices with FM1–43 in C. elegans, lamprey, and rat. Neuron *24*, 809–817.

Klingauf, J., Kavalali, E.T., and Tsien, R.W. (1998). Kinetics and regu-

lation of fast endocytosis at hippocampal synapses. Nature *394*, 581–585.

Kraszewski, K., Daniell, L., Mundigl, O., and Decamilli, P. (1996). Mobility of synaptic vesicles in nerve endings monitored by recovery from photobleaching of synaptic vesicle-associated fluorescence. J. Neurosci. *16*, 5905–5913.

Lagnado, L., Gomis, A., and Job, C. (1996). Continuous vesicle cycling in the synaptic terminal of retinal bipolar cells. Neuron *17*, 957–967.

Launay, P., Fleig, A., Perraud, A.L., Scharenberg, A.M., Penner, R., and Kinet, J.P. (2002). TRPM4 is a Ca^{2+}-activated nonselective cation channel mediating cell membrane depolarization. Cell *109*, 397–407.

Lenzi, D., Crum, J., Ellisman, M.H., and Roberts, W.M. (2002). Depolarization redistributes synaptic membrane and creates a gradient of vesicles on the synaptic body at a ribbon synapse. Neuron *36*, 649–659.

Luby-Phelps, K., Castle, P.E., Taylor, D.L., and Lanni, F. (1987). Hindered diffusion of inert tracer particles in the cytoplasm of mouse 3T3 cells. Proc. Natl. Acad. Sci. USA *84*, 4910–4913.

Mack, A.F., Behrens, U.D., and Wagner, H.J. (2000). Inhibitory control of synaptic activity in goldfish Mb bipolar cell terminals visualized by FM1–43. Vis. Neurosci. *17*, 823–829.

McNeil, P.L., and Terasaki, M. (2001). Coping with the inevitable: how cells repair a torn surface membrane. Nat. Cell Biol. *3*, E124–E129.

Meyers, J.R., MacDonald, R.B., Duggan, A., Lenzi, D., Standaert, D.G., Corwin, J.T., and Corey, D.P. (2003). Lighting up the senses: FM1–43 loading of sensory cells through nonselective ion channels. J. Neurosci. *23*, 4054–4065.

Morgans, C.W. (2000). Presynaptic proteins of ribbon synapses in the retina. Microsc. Res. Tech. *50*, 141–150.

Murthy, V.N., and Stevens, C.F. (1998). Synaptic vesicles retain their identity through the endocytic cycle. Nature *392*, 497–501.

Paillart, C., Li, J., Matthews, G., and Sterling, P. (2003). Endocytosis and vesicle recycling at a ribbon synapse. J. Neurosci. *23*, 4092–4099.

Pyle, J.L., Kavalali, E.T., Piedras-Renteria, E.S., and Tsien, R.W. (2000). Rapid reuse of readily releasable pool vesicles at hippocampal synapses. Neuron *28*, 221–231.

Rao-Mirotznik, R., Buchsbaum, G., and Sterling, P. (1998). Transmitter concentration at a three-dimensional synapse. J. Neurophysiol. *80*, 3163–3172.

Richards, D.A., Guatimosim, C., and Betz, W.J. (2000). Two endocytic recycling routes selectively fill two vesicle pools in frog motor nerve terminals. Neuron *27*, 551–559.

Richards, D.A., Guatimosim, C., Rizzoli, S.O., and Betz, W.J. (2003). Synaptic vesicle pools at the frog neuromuscular junction. Neuron *39*, 529–541.

Rieke, F., and Schwartz, E.A. (1996). Asynchronous transmitter release: control of exocytosis and endocytosis at the salamander rod synapse. J. Physiol. *493*, 1–8.

Ripps, H., Shakib, M., and MacDonald, E.D. (1976). Peroxidase uptake by photoreceptor terminals of the skate retina. J. Cell Biol. *70*, 86–96.

Rouze, N.C., and Schwartz, E.A. (1998). Continuous and transient vesicle cycling at a ribbon synapse. J. Neurosci. *18*, 8614–8624.

Ryan, T.A. (2001). Presynaptic imaging techniques. Curr. Opin. Neurobiol. *11*, 544–549.

Ryan, T.A., Smith, S.J., and Reuter, H. (1996). The timing of synaptic vesicle endocytosis. Proc. Natl. Acad. Sci. USA *93*, 5567–5571.

Schacher, S., Holtzman, E., and Hood, D.C. (1976). Synaptic activity of frog retinal photoreceptors. A peroxidase uptake study. J. Cell Biol. *70*, 178–192.

Schaeffer, S.F., and Raviola, E. (1978). Membrane recycling in the cone cell endings of the turtle retina. J. Cell Biol. *79*, 802–825.

Slepnev, V.I., and De Camilli, P. (2000). Accessory factors in clathrin-dependent synaptic vesicle endocytosis. Nat. Rev. Neurosci. *1*, 161–172.

Stevens, C.F., and Williams, J.H. (2000). "Kiss and run" exocytosis at hippocampal synapses. Proc. Natl. Acad. Sci. USA *97*, 12828–12833.

Takei, K., Mundigl, O., Daniell, L., and De Camilli, P. (1996). The synaptic vesicle cycle: a single vesicle budding step involving clathrin and dynamin. J. Cell Biol. *133*, 1237–1250.

Teng, H., and Wilkinson, R.S. (2000). Clathrin-mediated endocytosis near active zones in snake motor boutons. J. Neurosci. *20*, 7986–7993.

von Gersdorff, H., and Matthews, G. (1997). Depletion and replenishment of vesicle pools at a ribbon-type synaptic terminal. J. Neurosci. *17*, 1919–1927.

von Gersdorff, H., and Matthews, G. (1999). Electrophysiology of synaptic vesicle cycling. Annu. Rev. Physiol. *61*, 725–752.

von Gersdorff, H., Vardi, E., Matthews, G., and Sterling, P. (1996). Evidence that vesicles on the synaptic ribbon of retinal bipolar neurons can be rapidly released. Neuron *16*, 1221–1227.

Von Kriegstein, K., Schmitz, F., Link, E., and Sudhof, T.C. (1999). Distribution of synaptic vesicle proteins in the mammalian retina identifies obligatory and facultative components of ribbon synapses. Eur. J. Neurosci. *11*, 1335–1348.

Zenisek, D., Steyer, J.A., Feldman, M.E., and Almers, W. (2002). A membrane marker leaves synaptic vesicles in milliseconds after exocytosis in retinal bipolar cells. Neuron *35*, 1085–1097.

Zucker, R.S., and Regehr, W.G. (2002). Short-term synaptic plasticity. Annu. Rev. Physiol. *64*, 355–405.